SciMedCentral

JSM Nanotechnology & Nanomedicine

Research Article

The Effect of Silver Nanoparticle Size and Coating on *Escherichia coli*

Tajkarimi, M.[1], Iyer, D.[1], Tarrannum, M.[1], Cunningham, Q.[2], Sharpe, I.[3], Harrison, S. H.[2] and Graves, J. L.[1]

[1]*Department of Nanoengineering, North Carolina Agricultural and Technical State University, USA*

[2]*Department of Biology, North Carolina Agricultural and Technical State University, USA*

[3]*Department of Chemical, Biological, and Bioengineering, North Carolina Agricultural and Technical State University, US*

Special Issue on

Research at the Joint School of Nanoscience and Nanoengineering

***Corresponding author**

Joseph L. Graves, Jr., Associate Dean for Research & Professor of Biological Sciences, Joint School of Nanosciences and Nanoengineering, North Carolina A&T State University & UNC Greensboro, NC 27401, USA, E-mail: gravesjl@ncat.edu

Submitted: 18 July 2014

Accepted: 27 August 2014

Published: 29 August 2014

Keywords

- Nanoparticles
- *E. coli*
- AgNps

Abstract

Silver nanoparticles are being increasingly used as antimicrobials. The shapes, sizes, and coatings of silver nanoparticles are factors known to individually influence the release of silver ions (Ag+) and thereby their effectiveness. However, size and coating effects have not been investigated in combination. This experiment investigates the effect of size and coating of spherical silver nanoparticles specifically 10 nm spherical (citrate-coated, polyvinylpyrrolidone --PVP-coated), 40nm spherical (citrate-coated, PVP-coated) and bulk silver nitrate on the gram-negative bacterium *Escherichia coli*. We found that citrate coatings and smaller sizes of silver nanoparticles had significantly higher antimicrobial effect against *Escherichia coli* MG1655 compared to larger PVP-coated nanoparticles, while bulk silver nitrate was most effective. Thus, with regard to a gram-negative bacterium, the positively-charged citrate coating was more effective than the negatively-charged PVP coating. This indicates that care must be taken to determine the best type of silver nanoparticles to use against different bacterial species, and that the cellular composition and environment of bacteria may be expected to influence nanoparticle effectiveness.

INTRODUCTION

Emerging outbreaks of infectious disease and widespread resistance to conventional antimicrobial drugs are significant global public health problems, and there has been an increasingly aggressive search for new antimicrobial agents [1,2]. Nanoparticles have been proposed due to their high surface-to-volume ratio and their unique chemical and physical properties which are often best realized through the use of metallic compounds [2-4]. In particular, silver is a metal that has had historical use as an antimicrobial agent [2,5-7]. Past examples of the antimicrobial use of silver include its use for water treatment in 1000 BCE, the use of silver nitrate to treat venereal disease in 1700 CE, and the use of silver nitrate to treat fresh burns from at least the 18th century forward [5-9]. In modern times, silver has been successfully used as an antimicrobial against 16 major species of bacteria.

The antimicrobial activity of silver has been established to be due to Ag+ ions in a number of studies going back at least to the 1970's. For example, Spadaro et al. [10] utilized silver electrodes with weak direct current to inhibit growth on agar plates for the bacterial varieties of *Staphylococcus aureus*, *Escherichia coli*, *Proteus vulgaris*, and *Pseudomonas aeruginosa*. These results are particularly interesting in that the strains used in this study were isolated from patients in the Veterans Administration Hospital in Syracuse, NY. Strains living in hospitals have been exposed to a number of biocidals and in general should be "tougher" than stains living in the general environment. Indeed, silver-resistant bacteria have been repeatedly found in burn wards, clinical and natural environments, and on human teeth [11].

Sondi and Salopek-Sondi [12] is one of the earliest studies that examined specifically the impact of silver nanoparticles on bacterial growth. Their study with *E.coli* and 12 nm diameter nanoparticles suggested that if the primary mechanism of biocidal action is Ag+ ions, then AgNPs would be more effective than bulk silver. In all treatments (10, 50, and 100 μg/cm^3), there was a significant delay in bacterial growth and lower population size achieved at the end of 9 hours relative to the control (0 μg/cm^3). The effect was greatest for 100 μg/cm^3 with exponential growth delayed for an additional hour, and a final population

size of 42% (0.75 x 10^9colony forming units; CFU) relative to the control. Sondi and Salopek-Sondi [12] argued that this was due to the fact that the concentration of the AgNPs decreased with time in the culture. This resulted from the interaction of the AgNPs with the intracellular substances of the destroyed cells. Their SEM images showed that AgNPs coagulated with dead bacterial cells, thus reducing the concentration of them and Ag+ ions in the liquid medium. Subsequent studies have confirmed these general findings Baker et al. [13]; Morones et al. [3]; Panacek et al. [14]; Pal et al. [15]; Shahverdi et al. [16]; among others. These impacts of AgNPs have also been found for natural microbial communities [17-19].

Nanoparticle morphology is an important determinant of toxicity to bacteria with smaller NPs being most effective [13,14]. Morones et al. [3] studied NPs in the range of 1 – 100 nm diameters and found that toxicity was enhanced based on a lower size range (1 – 10 nm), and observed a range of varying NP shapes through transmission electron microscopy (TEM). Pal et al. [16] found that truncated triangular AgNPs displayed the greatest effect on *E. coli* compared to spherical and rod-shaped NPs.

While the exact mechanisms of silver nanoparticle toxicity to bacteria are not fully known, there is a growing consensus concerning the candidate actions. First, the action of silver nanoparticles occurs both by the release of silver ion (Ag+) as well as from potential disruption or damage to the cell wall and membrane caused by the particles themselves [2,11,20]. Silver interacts with the thiol group compounds found in respiratory enzymes of bacterial cells. It also binds to the bacterial cell wall and cell membrane inhibiting the respiration process [3,9]. Silver is known to act on *E. coli* by inhibiting the uptake of phosphorous and releasing phosphate, manitol, succinate, proline, and glutamine from the cells [20,21]. The penetration of silver ions inside the cell is thought to impact the ability of DNA to replicate by causing it to condense. Furthermore, silver ions may interact with the thiol groups of proteins inside the cell causing these to become inactivated [20,22,23]. Due to the large surface area to volume ratio, smaller AgNPs should be able to more effectively release Ag+ ions into the cell and, following attachment to the cell membrane, may also penetrate into the cell [3, 11, 14-16, 20]. Once inside, Ag+ ions may be lethal as they disrupt metabolism, cell signaling, DNA replication, transcription, translation, and cell division, either directly or through the generation of reactive oxygen species (ROS) [11,20]. In summary, the toxicity of AgNPs upon bacteria appears dependent on particle shape, size, and concentration (> 75 μg/ml usually ceases growth) [20]. This study investigates the effect of AgNP on bacteria by examining both particle size and coating type. AgNPs can be synthesized both by chemical and biological methods [16,24-26]. Chemical methods require some sort of compound coating the AgNPs to prevent further aggregation. For example, Sondi, Goia, and Metijevic [24] utilized Daxad 19, a sodium salt of high molecular weight naphthalene sulfonate formaldehyde to prevent NP aggregation. Others have used citrate ($C_6H_5Na_3O_7$), thiosalicyclic acid ($C_6H_4(SH)CO_2H$, IUPAC name, 2-mercaptobenzoic acid), or polyvinylpyrrolidone (PVP, IUPAC name 1-ethenylpyrrolidin-z-one) as coating agents for AgNP production. The fact that these coatings have different solubility's would impact solution pH differently, may adhere to biological cell walls differently suggests that coating type may play a role in how AgNPs kill bacteria. El Badaway et al. [27] showed that toxicity of AgNPs was dependent on more negatively charged particles. In a study performed on *Bacillus* spp, they found toxicity increased along the following series of coatings: uncoated (H_2—AgNPs), citrate coated (Citrate-AgNPs), polyvinylpyrrolidone coated (PVP-AgNPs), and branched polyethyl-eneimine coated (BPEI-AgNPs). Our study will test the generality of this finding by specifically comparing two different commonly used coatings (citrate, PVP) and examine toxicity for 10 nm and 40 nm AgNPs in the model gram-negative bacterium *Escherichia coli*.

MATERIALS AND METHODS

Bacterial culture

We cultured *E. coli* K-12 MG1655 using Davis Minimal Broth (DMB, Difco™Sparks, MD) with Dextrose 10%(Dextrose, Fisher Scientific, Fair Lawn, NJ) as a sole carbon source, enriched with thyamine hydrochloride 0.1% (Thyamin Hydrochloride, Fisher scientific, Fair Lawn, NJ) in 10 ml of total culture volume maintained in 50 ml Erlenmeyer flasks. The flasks were placed in a shaking incubator with temperature maintained at 37°C for 24 hours. Cultures were propagated by daily transfers of 0.1 ml of each culture into 9.9 ml of DMB.

Measuring bacterial growth

Bacterial growth in BHI broth samples was assessed by measuring turbidity at 620 nm for hours 0, 3, 6, 12 and 24, using a 98-well plate Synergic Mx spectrophotometer (Biotek, VA USA) using clear polyester 98-well plates.

Bacterial enumeration

Bacterial populations were determined by spread plating on DMA agar. In this procedure, samples were withdrawn from inoculated samples at 0 and 24 h and were serially diluted in 0.1% peptone water. Appropriate dilutions were surfaced plated (200 μl) onto duplicate DMA plates.

SEM image bacterial preparation

SEM preparation was conducted using aldehyde fixative for a minimum of one hour using Karnovsky'sglutaraldehyde, followed by 2% paraformaldehye2% glutaraldehydein 0.1M phosphate buffer for another hour, post-fixation with osmium tetroxide and cacodylatephosphate buffer for one hour and washing with deionized water, followed by applying a series of graded acetonitrile using concentrations of 50,70,90,95, and 100%. We used Zeiss Auriga BUFIBFESEM.

AFM image bacterial preparation

Glass slides were washed carefully with acetone and then sonicated with 100% ethanol and deionized water for 10 minutes. The glass slide is dried with nitrogen gas and plasma cleaned for 3 minutes. Bacteria were washed for 10 minutes at 4°C with deionized water and 10 μl of 0.1% ploy – l -Lysin were added into the glass and the same volume of the washed bacteria were added and air dried. Imaging was then immediately conducted using tapping mode AFM [28].We used AFM Agilent model 5600LS.

Experimental design

The ability of the bacteria to grow in response to silver was determined by exposing them to varying concentrations of spherical silver nanoparticles of 10 nm and 40 nm diameter sizes, and of different coating, citrate and PVP (obtained from nano Composix, San Diego, CA) and bulk silver nitrate (Fisher Scientific, Fair Lawn, NJ). We determined that the different-sized silver nanoparticles and bulk silver nitrate were effective over different concentration ranges replicating the findings of earlier researchers [3]. Therefore we assayed the effectiveness of 10 nm particles at concentrations of 100 µg/L, 250 µg/L, 500 µg/L, 750 µg/L, and 1000 µg/L. The 40 nm particles were evaluated at 2000 µg/L, 4000µg/L, 5000µg/L, and 6000µg/L. Bulk silver nitrate was evaluated at 50 µg/L, 100 µg/L, 250 µg/L, 500 µg/L, 1000 µg/L, and 2000 µg/L. All silver treatments were compared to equivalent inoculates of bacteria growing in DMB medium without silver (control). Population growth in response to silver was measured by optical density and by determining colony forming units (CFU) via serial transfer on DMB agar plates at 0 and 24 hours. Two plates were prepared for each treatment in each experiment. The optical density was determined as an estimate of the cell density of bacteria at 620 nm absorbance using a multi-mode single-channel monochromator-based microplate reader. Optical density readings were taken at 0, 3, 6, 12, and 24 hours of growth. Optical density readings were recorded twice for each treatment in each experiment.

RESULTS

Figure 1 shows the population growth as measured by the mean optical density of the bacteria in the presence of 40 nm citrate-coated silver nanoparticles at varying concentrations relative to the control bacteria. The standard deviations in all optical density measurements ranged between 0.001 and 0.049, with a mean standard deviation of 0.005. Given these small values, none of the standard deviations are shown in there optical density figures. Figure 1 shows that there is no apparent growth of the bacteria at any of the concentrations assayed (2000, 4000, 5000, and 6000 µg/L). Table 1 reports the differences in the natural logarithms of CFUs at 0 and 24 hours for all experiments reported on in this study. In all treatments containing 40nm citrate-coated nanoparticles, the difference between CFUs is negative, while the control treatment showed substantial positive growth in CFU's (increasing by over 1 log unit in 24 hours). The difference was concentration dependent, with the greatest differences occurring at concentrations exceeding 5000 µg/L (> -2.00 log units.) Figure 7a and show Scanning Electron Microscope (SEM) images of treated and non-treated bacteria with 40 nm PVP-coated silver nanoparticles. Figure 7b reports coagulations of silver nanoparticles on the surface of bacteria compared to non-treated bacteria. Figure 8a and b compare the AFM image of non-treated and treated bacterial with AgNPs. This image was taken using the tapping mode [28] both of these images illustrate association of silver nanoparticles with the bacterial cell wall compared to the control treatment without silver nanoparticles. The AFM image of the treated cell shows apparent damage to the cell wall compared to the untreated control.

Table 2 reports the intrinsic rates of increase for the bacteria from all experiments at different concentrations of the various nanoparticles and bulk silver nitrate. The intrinsic rate of

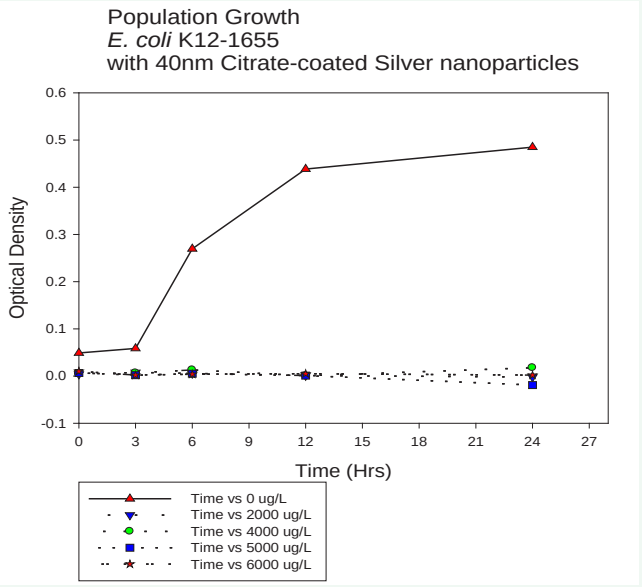

Figure 1 Shows population growth as measured by optical density of bacterial cultures exposed to 40nm citrate-coated silver nanoparticles. Concentrations assayed were 0, 2000, 4000, 5000, and 6000 µg/L. Bacterial growth is eradicated at all concentrations greater than 0 µg/L.

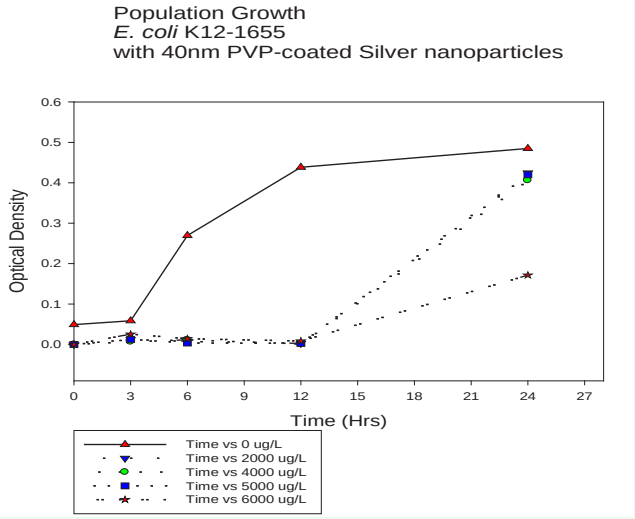

Figure 2 Shows population growth as measured by optical density of bacteria exposed to 40nm PVP-coated silver nanoparticles. Concentrations assayed were 0, 2000, 4000, 5000, and 6000 µg/L.

increase, r, is calculated using the standard exponential growth equation:

$N_t = N_0 * e^{rT}$;

Thelinear form is:

$\ln(N_t) = \ln(N_0) + rT$

where N_t is the population size at 24 hours measured by CFUs, N_0 is the population size at 0 hours measured by CFUs, T is time in hours, and r is the intrinsic rate of increase.

Table 1: Ln of CFU difference by experiment and treatment.

40nm Citrate-coated				
Control	**2000**	**4000**	**5000**	**6000**
2.40	-1.75	-3.97	-5.12	-5.12
2.26	-1.84	-4.08	-5.23	-2.23
40nm PVP-coated				
Control	**2000**	**4000**	**5000**	**6000**
2.04	1.37	0.64	1.48	0.83
2.26	1.26	0.81	1.32	0.73

10nm Citrate-coated					
Control	**100**	**250**	**500**	**750**	**1000**
2.26.981	1.91	1.14	-2.21	-4.29	-2.90
2.23	2.11	1.03	-2.17	-4.11	-2.973
10nm PVP-coated					
Control	**100**	**250**	**500**	**750**	**1000**
2.26	1.87	-0.68	-1.38	-1.80	-2.42
2.23	1.80	-0.79	-1.39	-1.83	-2.49

Bulk Silver Nitrate						
Control	**50**	**100**	**250**	**500**	**1000**	**2000**
2.17	1.86	-2.65	-4.15	-6.45	-7.60	-7.60
2.16	1.90	-2.09	-4.14	-6.44	-7.59	-7.59

(All concentrations are in µg/L)

Differences in ln CFU units are given for each treatment (concentrations) and experiment. These show that for 40 nm particles Citrate-coating is more effective than PVP-coating (greater log reduction at all concentrations.) At the 10 nm size, PVP performed best at 250 mg/L, but Citrate showed greater reduction at the higher concentrations.

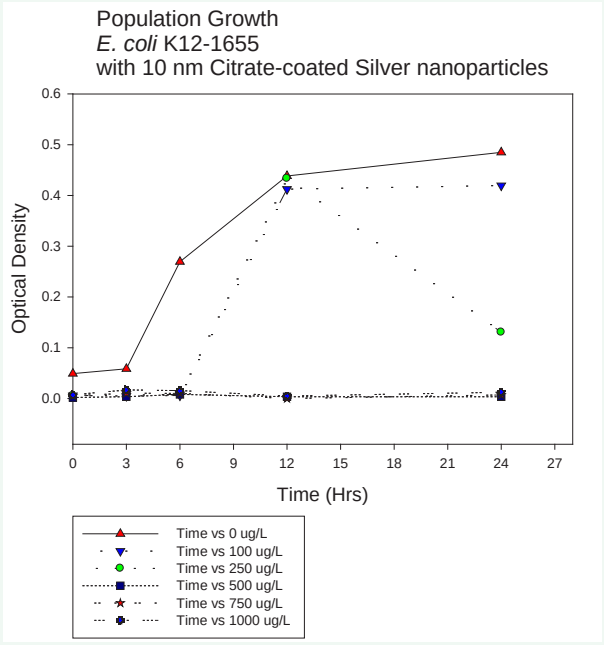

Figure 3 Shows population growth as measured by optical density of bacteria exposed to 10nm citrate-coated silver nanoparticles. Concentrations assayed were 0, 100, 250, 500, 750, and 1000 µg/L. Bacterial growth is eradicated at all concentrations greater than 250 µg/L. Population growth is delayed by six hours at concentrations of 100 and 250 µg/L respectively.

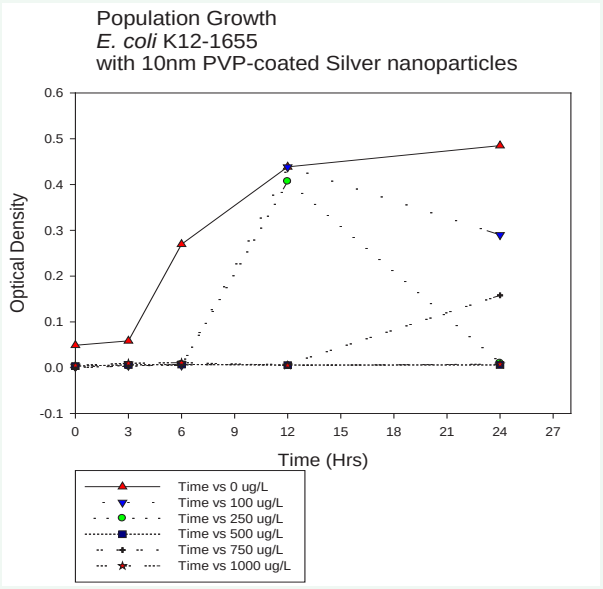

Figure 4 Shows population growth as measured by optical density of bacteria exposed to 10nm PVP-coated silver nanoparticles. Concentrations assayed were 0, 100, 250, 500, 750, and 1000 µg/L. Bacterial growth is eradicated at 1000µg/L. Bacterial growth is delayed by 6 hours and 12 hours at concentrations 100 and 250 µg/L and 500 and 750µg/L respectively.

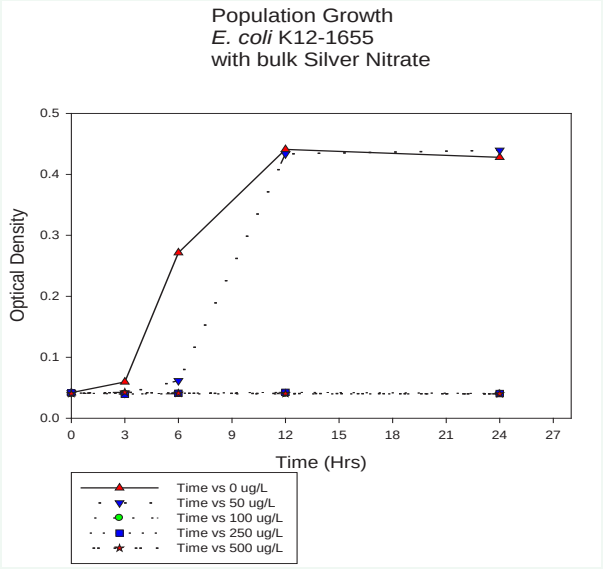

Figure 5 Shows population growth as measured by optical density of bacteria exposed to bulk silver nitrate. Concentrations assayed were 0, 100, 250, and 500 µg/L. Bacterial growth is eradicated at all concentrations greater than 50 µg/L. Bacterial growth is delayed by 3 hours at 50 µg/L.

Table 2 shows for the 40nm citrate-coated nanoparticles that for all treatments of these particles the value of r is negative. This follows automatically since the value of r is dependent on the difference in the ln CFU, which is negative in this experiment. The magnitude of r is concentration dependent, with the lowest values observed at the highest concentrations of nanoparticles. The

implication of this is that prolonged exposure of these bacteria to 40nm citrate-coated bacteria at the highest concentrations should cause extinction of the culture. It should also be noted that the concentrations of 40nm nanoparticles used (2000 – 6000 µg/L) to achieve these negative growth rates were much higher than for either 10nm or bulk silver.

Figure 2 shows that the bacteria can achieve some population growth in the presence of 40nm PVP-coated nanoparticles as measured by the mean optical density of the bacteria at the concentrations assayed (2000, 4000, 5000, and 6000 µg/L respectively.) There is a lag in the growth of the PVP-coated 40 nm treatments compared to the control. Growth does not begin in these treatments until after 12 hours. Table 1 reports the differences in the ln CFUs at 0 and 24 hours are all positive for this experiment. Again the control treatment showed the most substantial positive growth in CFU's (increasing by about 1 log unit in 24 hours). At each concentration the bacteria continue to grow; this is also concentration dependent, with the least amount of difference occurring at concentrations exceeding 2000 µg/L. As measured by optical density, the increases of concentrations of 2000 to 5000 µg/L are similar and bacterial growth at 6000 µg/L lags behind that of the lower concentrations at the end of 24 hours. This is contradicted by the more accurate CFU measurements which show an inconsistent pattern of population increase by concentration as shown in Tables 1 (CFU difference) and 2 (intrinsic rate of increase). These results allow a comparison of the efficacy of citrate- versus PVP-coated 40nm spherical nanoparticles. At this size and range of concentrations, citrate is more effective than PVP-coated nanoparticles for controlling bacterial growth.

Figure 3 illustrates that bacteria can achieve population growth in the presence of 10nm citrate-coated nanoparticles as measured by mean optical density of bacteria at the concentrations assayed (100, 250, 500, 750, and 1000 µg/L respectively). The results indicate that the smaller nanoparticles (10nm) are effective at a much lower concentration than the larger nanoparticles (40nm), per previous studies. At 100 and 250 µg/L, we observe a clear lag in the growth compared to the control (6 hours). Growth is effectively wiped out at the higher concentrations (500 – 1000 µg/L). The ln CFUs at 0 and 24 hours (Table 1) are positive for 100 and 250 µg/L and become negative at the higher concentrations. As in the previous experiments, this is concentration dependent via optical density measure, and inconsistent with concentration via the CFU measure. The highest reduction was observed at 750 µg/L (> -4.29), with 1000 mg/L showing somewhat less at (> -2.90).This is also mirrored in the inconsistent pattern of population increase by concentration as shown in (Table 2) (intrinsic rate of increase).

Figure 4 show the pattern of population growth in the presence of 10nm PVP-coated nanoparticles as measured by the mean optical density of the bacteria at the concentrations assayed (100, 250, 500, 750, and 1000 µg/L respectively). Again, as with citrate, the results indicate that the smaller PVP nanoparticles (10nm) are effective at a much lower concentration than the larger PVP nanoparticles (40nm), per previous studies. At 100 and 250 µg/L we again observe a clear lag in the bacterial growth compared to the controls (6 hours). Growth is effectively wiped out at the higher concentrations (500 – 1000 µg/L); except for an anomalous result at 750 µg/L. The optical density readings seem to indicate population growth at this population after 12 hours. The ln CFUs at 0 and 24 hours (Table 1) seem to contradict the observation of growth at the 750 µg/L treatment. All ln CFU differences are negative at concentrations higher than 100 µg/L for 10nm PVP-coated nanoparticles (Table 1) and all intrinsic rates of increase at these concentrations are negative as well (Table 2). The decrease in intrinsic rates of increase is highly concentration dependent in this experiment, so it is highly unlikely that the Figure 4 optical density spike at 24 hours in the 750 µg/L treatment is real. Finally, there is a notable different again (in the opposite direction) concerning the efficacy of citrate- versus PVP coated 10nm nanoparticles at 250 µg/L. At this concentration only, the PVP-coated particles are more effective than the citrate-coated. However, citrate-coated particles become more

Table 2: Intrinsic Rate of Increase (r) by experiment and treatment.

Citrate-coated 40nm					
	Control	**2000**	**4000**	**5000**	**6000**
Mean r	0.097	-0.075	-0.168	-0.216	-0.216
SD r	0.004	0.003	0.003	0.003	0.003
PVP-coated 40nm					
	Control	**2000**	**4000**	**5000**	**6000**
Mean r	0.097	0.055	0.030	0.058	0.033
SD r	0.004	0.003	0.005	0.005	0.003

Citrate-coated 10nm						
	Control	**100**	**250**	**500**	**750**	**1000**
Mean r	0.093	0.084	0.045	-0.091	-0.175	-0.122
SD r	0.001	0.006	0.003	0.001	0.005	0.002
PVP-coated 10nm						
	Control	**100**	**250**	**500**	**750**	**1000**
Mean r	0.093	0.076	-0.031	-0.058	-0.076	-0.102
SD r	0.001	0.002	0.003	0.000	0.001	0.002

Bulk Silver Nitrate							
	Control	**50**	**100**	**250**	**500**	**1000**	**2000**
Mean r	0.090	0.079	-0.099	-0.173	-0.269	-0.316	-0.316
SD r	0.000	0.001	0.016	0.000	0.000	0.000	0.000

(All concentrations are µg/L, all rates are per hour)

Table 3: Bulk Silver Nitrate, Non-Linear Regression – Concentration versus log CFU Difference.

r	**r^2**	**Adj. r^2**	**S.E. of Estimate**
0.930	0.876	0.853	0.669
Coefficient	**S.E.**	**t**	**p**
y_0= 0.409	0.284	1.44	<0.1772ns
a = -0.006	0.0001	-6.904	<0.0001
b = 2.56E-006	4.93E-007	5.199	0.0003

Table 3 shows the significance of the non-linear regression from Figure 6. While the intercept value (y0) is not significant, the parameters describing the descent and shape of the curve are highly significant (a, b.) This suggests that response of E. coli to bulk silver nitrate is highly dependent on concentration with diminishing returns at higher concentrations.

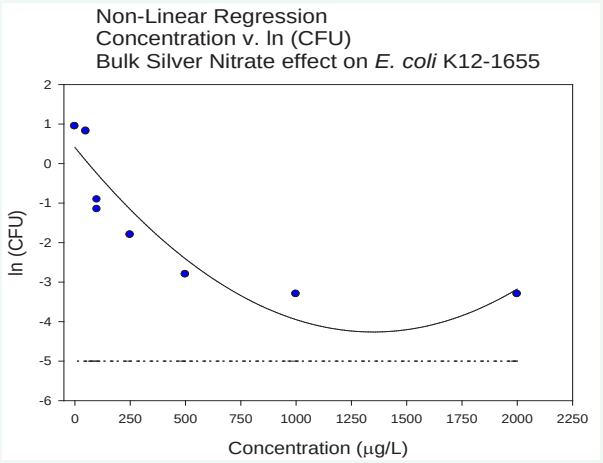

Figure 6 Difference in colony forming units (ln CFU) between the start of the exposure (0 hours) and the end of the exposure (24 hours) of bulk silver nitrate. The dashed line indicates a five log reduction (Pasteurization level). This never occurs, but at concentrations > 500 µg/L a 3 log reduction is observed. Significant reductions (> 1-- 2 logs) were observed at all concentrations greater than 50 µg/L. The non-linear regression was highly significant (see Table 3).

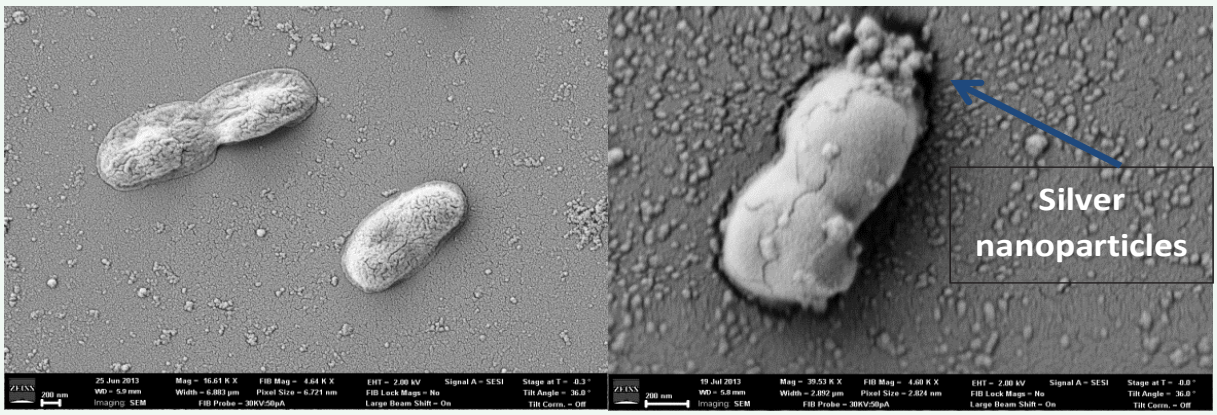

Figure 7 SEM images of E. coli MG1655. **(a)** Non-treated. **(b)** Treated with 20 µg/l 40 nm PVP coated spherical silver nanoparticles. Silver nanoparticle accumulation is apparent on the surface of the treated bacterial cell.

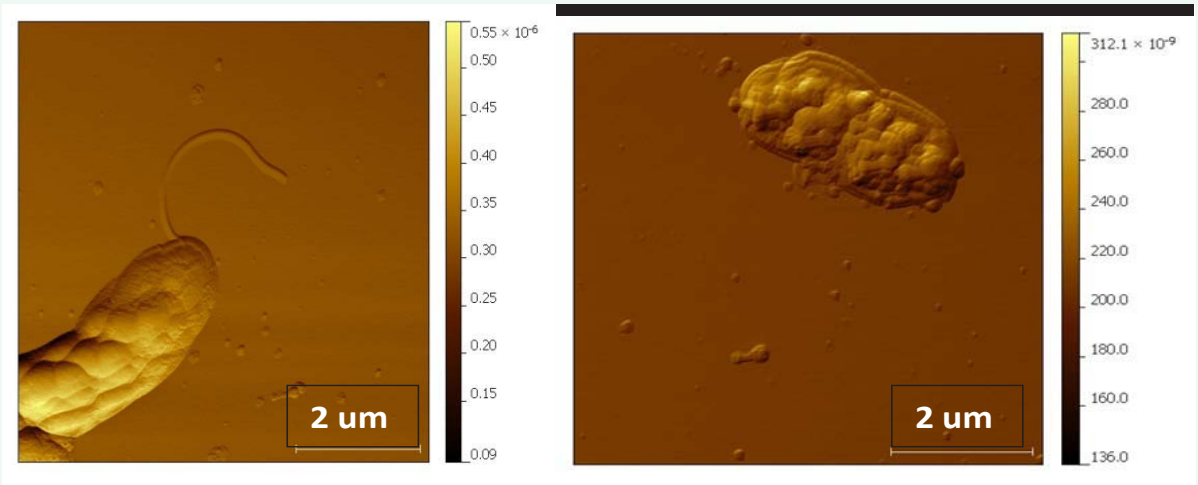

Figure 8 AFM images of *E. coli* MG1655. **(a)** Non-treated. (b) Treated with 250 µg/l 10 nm citrate-coated spherical silver nanoparticles. There is a distinctive surface change on cell wall structure in response to treatment.

effective (~2X) in reducing bacterial population size at all higher concentrations (500 –1000µg/L).

Figure 5 shows the pattern of population growth in the presence of bulk silver nitrate as measured by the mean optical density of the bacteria at the concentrations assayed (50, 100, 250, 500, 1000, and 2000 µg/L respectively). These ranges were chosen to allow comparison of the effectiveness of bulk silver nitrate versus both the 10 and 40nm nanoparticles. The results show that bulk silver nitrate can effectively control bacterial growth at >100 µg/L, superior to the 10nm nanoparticles. There is a three hour lag in bacterial growth compared to the controls at a concentration of 50 µg/L. Bacterial growth is effectively wiped out at the higher concentrations (100 – 2000 µg/L). The ln CFUs at 0 and 24 hours (Table 1) are consistent and show a strong relationship with concentration (Figure 6). This relationship has the form of diminishing returns, with concentrations higher than 500 reducing the cultures by > 6 ln units. As expected, all intrinsic rates of increase at concentrations higher than 50 µg/L are negative and highly concentration dependent as well (Table 2).These data all together indicate that the efficacy of the various silver treatments with regard to minimum concentration required to eliminate bacterial growth are PVP-coated 40nm <citrate-coated 40nm <citrate-coated 10nm < PVP-coated 10nm, and most effective was bulk silver nitrate. The relationship between PVP-coated and citrate-coated 10nm particles reverses at concentrations higher than 250 µg

DISCUSSION

This study tested the generality of the efficacy of two commonly used coatings (citrate, PVP) and their interaction with size (10 and 40 nm) spherical silver nanoparticles and compared their impact across a range of concentrations to that of bulk silver in a gram-negative bacterium, *Escherichia coli K12* MG1655. One of the earliest studies of the impact of silver nanoparticles on *E. coli* is Sondi and Salopek-Sondi [12]. They prepared their nanoparticles from silver nitrate solution, and washed them to remove surfactant (coating) before exposing bacteria *E. coli* strain. The modal size of their nanoparticles was ~12nm. The range of concentrations used to assay the bactericidal effects of these nanoparticles in liquid Luria-Bertani (LB) medium was 10, 50, and 100 µg/cm; converted to our scale: 10,000, 50,000, and 100,000 µg/L. Their results indicated that cells of *E. coli* strain B under these conditions were capable of growing at all these concentrations, although the growth curves were delayed and lowered in magnitude with increasing silver nanoparticle concentration. Given our results and that of subsequent studies, it is hard to imagine that 12nm nanoparticles allowed bacterial growth at these concentrations. In the discussion of this paper, the authors claimed that silver nanoparticles, even at high concentrations, only caused growth delay in liquid medium. They suggested that over time the concentration of nanoparticles gradually decreased due to the interaction of the nanoparticles with the intracellular substances of the destroyed cells. Their evidence for this was SEM imaging showing nanoparticles associated with dead cells. While this might be true, it is noticeable that the materials and methods in this paper did not mention whether the liquid cultures were maintained using a shaking incubator (as in our study). While our study did not test the efficacy of nanoparticles in liquid media that is stagnant versus mixing, it is highly likely that the former is much less effective through time compared to the latter.

Yoon et al. [29] evaluated the efficacy of silver and copper nanoparticles (25—65, mode 40nm and 40—140, mode ~90) on *E. coli* and the closely related bacterium *Bacillus subtilis* utilizing LB and nutrient agar plates respectively. These nanoparticles were obtained from ABC Nanotech Co. Ltd. and Nano Technology Inc. They did not report in their materials and methods whether these were coated, or what the coatings were. The silver nanoparticle concentrations used to achieve 90% bacterial reduction on these plates was 58.41 µg/mL for *E. coli* and 32.12 µg/mL for *B. subtilis.* Copper was more effective with lower concentrations required for 90% reduction at 33.49 µg/mL for *E. coli* and 28.20 µg/mL for *B. subtilis*. Our experiment did not test the effectiveness of citrate-coated and PVP-coated nanoparticles in agar, but work we are not publishing here using diffusion assays with these nanoparticles at much lower concentrations indicates that the Yoon et al. [29] figures are again orders of magnitude higher than required to achieve Pasteurization of bacteria. Another study [30] used silver nanoparticle ranging from 2 –8 nm and copper nanoparticles ranging from 6 –16 nm to evaluate their impact on a series of *E. coli* and *B. subtilis* strains. The shape of the nanoparticles was not reported but their TEM analysis showed them to be roughly spherical. They measured minimum inhibitory concentration (MIC) in liquid medium. MIC is considered the concentration that kills 99.9% of the bacteria in the culture. They found at range of MIC for *E. coli* strains in response to silver nanoparticles with the most sensitive are *E. coli* MTCC443 at 40 mg/mL and least sensitive being *E. coli* MTCC739 at 180 mg/mL. *E.coli* MTCC443 was also the most sensitive to copper at MIC of 140 mg/mL, while *E. coli* MTCC739 was among the most resistant to copper at MIC of 220 mg/L. It should be noticed that these results are opposite that of Yoon et al. 2006, which found *E. coli* more sensitive to silver than to copper.

At least one study has corroborated the impact of silver nanoparticles on *E. coli* at much lower concentrations than the studies summarized above [15]. This study used silver nanoparticles of different shapes and demonstrated that shape, as well as size mattered in nanoparticle efficiency. Pal et al. [15] used concentrations of 0.01µg/ml – 1 µg/ml (on our scale,10 µg/L – 1000 µg/L). These nanoparticles were assayed for their impact on bacterial growth in liquid medium (Difco nutrient broth, NB). Their liquid assays were conducted with shaking as well (better matching our conditions). They found that increasing the concentration of nanoparticles delayed bacterial growth, and at the highest concentrations essentially wiped it out (0.50 µg/mL, 1.00 µg/mL; equivalent to our scale at 500 µg/L and 1000 µg/L.) Our study found in all combinations of coating and size that at 500 µg/L bacterial growth was retarded or wiped out relative to controls and at 1000 µg/L all growth was wiped out (Table 1). El Badawy et al. [21] also measured the impact of surfactant coating on silver nanoparticles using concentrations similar to this study on the gram-positive bacterium *Bacillus* spp. (5 µg/L –1000 µg/L).They utilized spherical nanoparticles that varied in size range from 10 nm to 18 nm. Their study found that the more negatively charged the coating the more effective it was against *B. subtilis* (thus PVP > citrate in killing potential).

Our results partially corroborate this finding in this size range, as at a lower concentration 250 µg/L the 10nm size PVP-coated was more effective in reducing bacterial growth than the citrate-coated (Tables 1 & 2, Figures 3 & 4.) However, at the higher concentrations of this experiment, the 10 nm citrate-coated particles were much more effective than the PVP-coated and we also found the exact opposite result with our 40 nm sized nanoparticles. At 40nm, citrate-coated was much more effective than PVP-coated with regard to reducing bacterial growth. Table 1 shows that at 40 nm size a much greater concentration of nanoparticles were required and that PVP-coated did not stop bacterial growth at all, just slowed it relative to the control; whereas, at this size, citrate was effective at reducing bacterial population size at all concentrations. As an overall evaluation of the two against the gram-negative bacterium, *E. coli*, it seems that the more positively charged nanoparticle (citrate-coated) was the more effective. This suggests that nanoparticles will need to be tested more extensively across bacterial diversity to determine the best compositions and coatings to reduce bacterial growth.

This study also found that bulk silver was far more effective than all types of nanoparticles (size or coating) in reducing bacterial growth. Not only did bulk silver nitrate have greater effects at lower or equivalent concentrations, but the results were strongly predictable by concentration (Figure 6) in ways that the nanoparticle results were not. This is consistent with studies which suggest that the concentration of silver ion (Ag+) is the primary mechanism by which silver nanoparticles impart their effect on bacteria [5,6,11,20]. Before engineered nanoparticles were available, bacteriologists were studying the impact of metals and metallic oxides [10,32]. Spadaro et al. demonstrated that metal ions could strongly inhibit *E. coli*, *S. aureus*, *P. vulgaris*, and *P. aeruginosa*. Li, Nikaido, and Williams1997demonstrated that silver-resistant mutants of *E. coli* achieved this resistance by actively transporting Ag+ ions out of the cell. It is not a general rule however, that metal/metallic oxide ions are more toxic to bacteria than nanoparticles. Bandyopadhyay et al. [33] have shown that while cerium oxide (CeO^2) and Ce^{4+} ions have equivalent effects on the nitrogen fixing bacterium *Sinorhizobiummeliloti*, zinc (Zn) nanoparticles were far more toxic than Zn^{2+} ion. The zinc nanoparticles showed much greater toxicity to *S. melilioti* at all concentrations assayed (31, 62.5, and 125 ppm.)

Silver and Phung [31] show that such heavy metal transporting mechanisms are actually widespread in bacteria. *E.coli* K12 MG1655 was chosen for this study because it does not have specific silver resistance plasmids or chromosomal elements. Bacteria with such elements can show 100-fold greater MICs than those without [11,31]. This means that studies of the impact of metallic or metallic oxide nanoparticles should take care to be sure to know the resistance elements that might exist within the strains to be used in the study. For example, Planchon et al. [34] has shown that the cyanobacterium *Synechocystis* spp. produces an exopolysaccharide which offers it protection against damage induced by titanium dioxide nanoparticles. Mutants deficient in the ability to make the exopolysaccharide are far more vulnerable.

In summary, this study evaluated the toxicity of citrate-coated and PVP-coated nanoparticles of 40nm and 10nm and compared their toxicity to bulk silver nitrate against *E. coli* K12 MG1655. As in previous work, both size and coating of the nanoparticle impacted toxicity as measured by population growth (optical density and CFU) across a range of concentrations. Generally, we found that we could achieve significant population growth reduction against this strain with both sized and coated nanoparticles at orders of magnitude lower concentrations than shown in many previous studies. At the smallest size, the more negatively coated PVP nanoparticles had superior effect at a lower concentration, but the more positively charged citrate-coated particle performed best at higher concentrations. At the larger size, citrate coated nanoparticles were clearly superior in bacterial growth reduction. Bulk silver nitrate was more effective than all nanoparticles assayed. These results suggest that care must be taken with regard to choosing the most appropriate size, coating, and concentrations required to reduce bacterial populations even under well-defined laboratory conditions. This of course indicates that this problem will be even more difficult to address under more natural conditions (e.g mixed bacterial communities with widely circulating heavy metal resistance genetic elements). Our further studies will examine some of these complications more fully.

REFERENCES

1. Kate E. Jones, Nikkita G. Patel, Marc A. Levy, Adam Storeygard, Deborah Balk, John L. Gittleman, et al Global trends in emerging infectious diseases. Nature. 2008; 451: 990-993
2. Rai M, Yadav A, Gade A. Silver nanoparticles as a new generation of antimicrobials. Biotechnol Adv. 2009; 27: 76-83.
3. Morones JR, Elechiguerra JL, Camacho A, Holt K, Kouri JB, Ramírez JT, et al. The bactericidal effect of silver nanoparticles. Nanotechnology. 2005; 16: 2346-2353.
4. Kim JS, Kuk E, Yu KN, Kim JH, Park SJ, Lee HJ, et al. Antimicrobial effects of silver nanoparticles. Nanomedicine. 2007; 3: 95-101.
5. Silver S. Bacterial silver resistance: Molecular biology and uses and misuses of silver compounds. FEMS Microbiol Rev. 2003; 27: 341-353.
6. Xiu ZM, Zhang QB, Puppala HL, Colvin VL, Alvarez PJ. Negligible particle-specific antibacterial activity of silver nanoparticles. Nano Lett. 2012; 12: 4271-4275.
7. Prabhu S, Poulose E. Silver nanoparticles: Mechanism of antimicrobial action, synthesis, medical applications, and toxicity effects. International Nano Letters 2012; 2: 1-10.
8. Castellano JJ, Shafii SM, Ko F, Donate G, Wright TE, Mannari RJ, et al. Comparative evaluation of silver-containing antimicrobial dressings and drugs. Int Wound J. 2007; 4: 114-122.
9. Klasen HJ. A historical review of the use of silver in the treatment of burns. Part I early uses, Burns 2000; 30:1-9.
10. Spadaro JA, Berger TJ, Barranco SD, Chapin SE, Becker RO. Antibacterial effects of silver electrodes with weak direct current. Antimicrob Agents Chemother. 1974; 6: 637-642.
11. Mijnendonckx K, Leys N, Mahillon J, Silver S, Van Houdt R. Antimicrobial silver: uses, toxicity and potential for resistance. Biometals. 2013; 26: 609-621.
12. Sondi I, Salopek-Sondi B. Silver nanoparticles as antimicrobial agent: a case study on E. coli as a model for Gram-negative bacteria. J Colloid Interface Sci. 2004; 275: 177-182.
13. Baker C, Pradhan A, Pakstis L, Pochan DJ, Shah SI. Synthesis and antibacterial properties of silver nanoparticles. J Nanosci Nanotechnol.

2005; 5: 244-249.

14. Panacek A, Kvítek L, Prucek R, Kolar M, Vecerova R, Pizúrova N, et al. Silver colloid nanoparticles: synthesis, characterization, and their antibacterial activity. J Phys Chem B. 2006; 110: 16248-16253.

15. Pal S, Tak YK, Song JM. Does the antibacterial activity of silver nanoparticles depend on the shape of the nanoparticle? A study of the Gram-negative bacterium Escherichia coli. Appl Environ Microbiol. 2007; 73: 1712-1720.

16. Shahverdi AM, Fakhimi A, Shahverdi HR. Minaian S. Synthesis and effect of silver nanoparticles on the antibacterial activity of different antibiotics against Staphyloccoccus aureus and Escherichia coli, Nanomedicine, Nanotechnology, Biology, and Medicine 2007; 3: 168—171.

17. Burchardt AD, Carvalho RN, Valente A, Nativo P, Gilliland D, Garcìa CP, et al. Effects of silver nanoparticles in diatom Thalassiosira pseudonana and cyanobacterium Synechococcus sp. Environ Sci Technol. 2012; 46: 11336-11344.

18. García A, Delgado L, Torà JA, Casals E, González E, Puntes V, et al . Effect of cerium dioxide, titanium dioxide, silver, and gold nanoparticles on the activity of microbial communities intended in wastewater treatment. J Hazard Mater. 2012; 199-200: 64-72.

19. Merrifield DL, Shaw BJ, Harper GM, Saoud IP, Davies SJ, Handy RD, et al. Ingestion of metal-nanoparticle contaminated food disrupts endogenous microbiota in zebrafish (Danio rerio). Environ Pollut. 2013; 174: 157-163.

20. Rai MK, Deshmukh SD, Ingle AP, Gade AK. Silver nanoparticles: the powerful nanoweapon against multidrug-resistant bacteria. J Appl Microbiol. 2012; 112: 841-852

21. Yamanaka M, Hara K, Kudo J. Bactericidal actions of a silver ion solution on Escherichia coli, studied by energy-filtering transmission electron microscopy and proteomic analysis. Appl Environ Microbiol. 2005; 71: 7589-7593.

22. Liau SY, Read DC, Pugh WJ, Furr JR, Russell AD. Interaction of silver nitrate with readily identifiable groups: relationship to the antibacterial action of silver ions. Lett Appl Microbiol. 1997; 25: 279-283.

23. Feng QL, Wu J, Chen GQ, Cui FZ, Kim TN, Kim JO. A mechanistic study of the antibacterial effect of silver ions on Escherichia coli and Staphylococcus aureus. J Biomed Mater Res. 2000; 52: 662-668.

24. Sondi I, Goia DV, MatijeviÄ‡ E. Preparation of highly concentrated stable dispersions of uniform silver nanoparticles. J Colloid Interface Sci. 2003; 260: 75-81.

25. Birla SS, Tiwari VV, Gade AK, Ingle AP, Yadav AP, Rai MK. Fabrication of silver nanoparticles by Phoma glomerata and its combined effect against Escherichia coli, Pseudomonas aeruginosa, and Staphylococcus aureus, Letters in Applied Microbiology 2009; 48: 173-179.

26. Wu, R-T and Hsu, S. L-U, Preparation of highly concentrated and stable suspensions of silver nanoparticles by an organic base catalyzed reduction reaction. Materials Research Bulletin, 2008; 43: 1276-1281.

27. El Badawy AM, Silva RG, Morris B, Scheckel KG, Suidan MT, Tolaymat TM. Surface charge-dependent toxicity of silver nanoparticles. Environ Sci Technol. 2011; 45: 283-287.

28. Camesano TA, Natan MJ, Logan BE. Observation of Changes in Bacterial Cell Morphology Using Tapping Mode Atomic Force Microscopy, Langmuir , 2000; 16: 4563-4572.

29. Yoon KY, Hoon Byeon J, Park JH, Hwang J. Susceptibility constants of Escherichia coli and Bacillus subtilis to silver and copper nanoparticles. Sci Total Environ. 2007; 373: 572-575.

30. Ruparelia JP, Chatterjee AK, Duttagupta SP, Mukherji S . Strain specificity in antimicrobial activity of silver and copper nanoparticles. Acta Biomater. 2008; 4: 707-716.

31. Silver S, Phung le T. A bacterial view of the periodic table: genes and proteins for toxic inorganic ions. J Ind Microbiol Biotechnol. 2005; 32: 587-605.

32. Li XZ, Nikaido H, Williams KE. Silver-resistant mutants of Escherichia coli display active efflux of Ag+ and are deficient in porins. J Bacteriol. 1997; 179: 6127-6132.

33. Bandyopadhyay S, Peralta-Videa JR, Plascencia-Villa G, Jose-Yacaman M, Gardea-Torresdey JL. Comparative toxicity assessment of CeO2 and ZnO nanoparticles towards Sinorhizobium meliloti, a symbiotic alfalfa associated bacterium: Use of advanced microscopic and spectroscopic techniques, J. Hazardous Materials, 2012; 241-242: 379- 386.

34. Planchon M, Jittawuttipoka T, Cassier-Chauvat C, Guyot F, Gelabert A, Benedetti MF, et al. Exopolysaccharides protect Synechocystis against the deleterious effects of titanium dioxide nanoparticles in natural and artificial waters. J Colloid Interface Sci. 2013; 405: 35-43.

35. Bondarenko O, Ivask a, Käkinen a, Kurvet I, Kahru A. Particle-cell contact enhances antibacterial activity of silver nanoparticles. PLoS One. 2013; 8: e64060.

36. Chait R, Vetsigian K, Kishony R. What counters antibiotic resistance in nature? Commons below Nat Chem Biol. 2011; 8: 2-5.

37. Choi O, Yu CP, Esteban Fernández G, Hu Z . Interactions of nanosilver with Escherichia coli cells in planktonic and biofilm cultures. Water Res. 2010; 44: 6095-6103.

38. Mathews KH (2001) Antimicrobial Drug Use and Veterinary Costs in U.S. Livestock Production. USDA.

Cite this article

Tajkarimi M, Iyer D, Tarrannum M, Cunningham Q, Sharpe I, et al. (2014) The Effect of Silver Nanoparticle Size and Coating on Escherichia coli. JSM Nanotechnol Nanomed 2(2): 1025.